End of the Little Ice Age in the Alps forced by industrial black carbon

Thomas H. Painter[a,1], Mark G. Flanner[b], Georg Kaser[c], Ben Marzeion[c], Richard A. VanCuren[d], and Waleed Abdalati[e]

[a]Jet Propulsion Laboratory, California Institute of Technology, Pasadena, CA 91109; [b]Department of Atmospheric, Oceanic, and Space Sciences, University of Michigan, Ann Arbor, MI 48109; [c]Institute of Meteorology and Geophysics, University of Innsbruck, 6020 Innsbruck, Austria; [d]Air Quality Research Center, University of California, Davis, CA 95616; and [e]Earth Science and Observation Center, Cooperative Institute for Research in Environmental Sciences, Boulder, CO 80309

Edited by Susan Solomon, Massachusetts Institute of Technology, Cambridge, MA, and approved July 19, 2013 (received for review February 19, 2013)

Glaciers in the European Alps began to retreat abruptly from their mid-19th century maximum, marking what appeared to be the end of the Little Ice Age. Alpine temperature and precipitation records suggest that glaciers should instead have continued to grow until circa 1910. Radiative forcing by increasing deposition of industrial black carbon to snow may represent the driver of the abrupt glacier retreats in the Alps that began in the mid-19th century. Ice cores indicate that black carbon concentrations increased abruptly in the mid-19th century and largely continued to increase into the 20th century, consistent with known increases in black carbon emissions from the industrialization of Western Europe. Inferred annual surface radiative forcings increased stepwise to 13–17 $W{\cdot}m^{-2}$ between 1850 and 1880, and to 9–22 $W{\cdot}m^{-2}$ in the early 1900s, with snowmelt season (April/May/June) forcings reaching greater than 35 $W{\cdot}m^{-2}$ by the early 1900s. These snowmelt season radiative forcings would have resulted in additional annual snow melting of as much as 0.9 m water equivalent across the melt season. Simulations of glacier mass balances with radiative forcing-equivalent changes in atmospheric temperatures result in conservative estimates of accumulating negative mass balances of magnitude −15 m water equivalent by 1900 and −30 m water equivalent by 1930, magnitudes and timing consistent with the observed retreat. These results suggest a possible physical explanation for the abrupt retreat of glaciers in the Alps in the mid-19th century that is consistent with existing temperature and precipitation records and reconstructions.

aerosol | cryosphere | albedo | climate

Between the end of the 13th and the middle of the 19th centuries, glaciers in the European Alps were considerably larger than at present (1). Beginning around 1865, however, glaciers across the Alps retreated rapidly to lengths generally shorter than in the known range of the previous 500 y (1), continuing to present day with interruptions by only minor advances (Fig. 1). This relatively abrupt retreat from the mid-19th century maximum is often considered by glaciologists to be the end of the Little Ice Age (LIA) (1–3).

Glaciologists have conjectured that increasing temperatures (4) and decreasing precipitation (2) caused the rapid observed retreat of glaciers throughout the Alps in the second half of the 19th century. However, such scenarios are inconsistent with temperature records and climate proxies for the Alps (5, 6). During the latter half of the 19th century and early 20th century, when glaciers were retreating rapidly, temperatures in the Alpine region were apparently cooler than in the late 18th to early 19th centuries (Fig. 2) and precipitation was largely unchanged (5–7). Glaciers subject to these climate forcings alone would have had positive mass balance and advanced (8), rather than retreated, as observed.

The density of temperature and precipitation observations in the Alps before 1800 was less than one-third that after 1860, by which time the density reached near its current level (5). Nevertheless, with our current knowledge of the Alpine climate, climatologists consider the climatic end of the LIA to have come markedly later than the glaciological end, resulting in a paradox (2).

Simulations of glacier-length variations using glacier flow and mass balance models forced with instrumental and proxy temperature and precipitation fail to match the timing and magnitude of the observed late 19th century retreat (8–12). Matches between simulations and observations have only been achieved when additional glacier mass loss is imposed after 1865, or when precipitation signals are generated that would fit the glacier retreat rather than using actual precipitation records (8, 10, 12, 13). Therefore, explaining the glacier retreat with climatic variables requires climate forcings that are inconsistent with the observations and reconstructions.

Huybrechts et al. (10) wrote plainly to the LIA discrepancy between glaciers and climate when modeling the glacier-length record of the Glacier d'Argentiere: "Forcing the mass balance history [with summer and mean annual temperature anomalies] brought to light, that, in particular, the observed glacier retreat since about 1850 is not fully understood. This result and the improved model simulations that could be obtained while assuming an additional negative mass balance perturbation during roughly the last 150 y, *seems to point to additional features affecting the glacier's mass balance that are not captured well in the ambient climatic records*" [italics added for emphasis] (10). In other words, Huybrechts et al. (10) suggest that some forcing beyond changes in temperature and precipitation was driving a large part of the negative mass balance.

Glacier mass balance is controlled by accumulation at higher elevations and ablation at lower elevations. In each year, glacier melt increases dramatically when snow cover melts completely, exposing the darker glacier ice to markedly increased energy fluxes. Therefore, any forcing that removes snow cover earlier in

Significance

The end of the Little Ice Age in the European Alps has long been a paradox to glaciology and climatology. Glaciers in the Alps began to retreat abruptly in the mid-19th century, but reconstructions of temperature and precipitation indicate that glaciers should have instead advanced into the 20th century. We observe that industrial black carbon in snow began to increase markedly in the mid-19th century and show with simulations that the associated increases in absorbed sunlight by black carbon in snow and snowmelt were of sufficient magnitude to cause this scale of glacier retreat. This hypothesis offers a physically based explanation for the glacier retreat that maintains consistency with the temperature and precipitation reconstructions.

Author contributions: T.H.P., M.G.F., G.K., B.M., and W.A. designed research; T.H.P., M.G.F., and B.M. performed research; T.H.P., M.G.F., and B.M. analyzed data; and T.H.P., M.G.F., G.K., B.M., R.A.V., and W.A. wrote the paper.

The authors declare no conflict of interest.

This article is a PNAS Direct Submission.

Freely available online through the PNAS open access option.

[1]To whom correspondence should be addressed. E-mail: Thomas.Painter@jpl.nasa.gov.

This article contains supporting information online at www.pnas.org/lookup/suppl/doi:10.1073/pnas.1302570110/-/DCSupplemental.

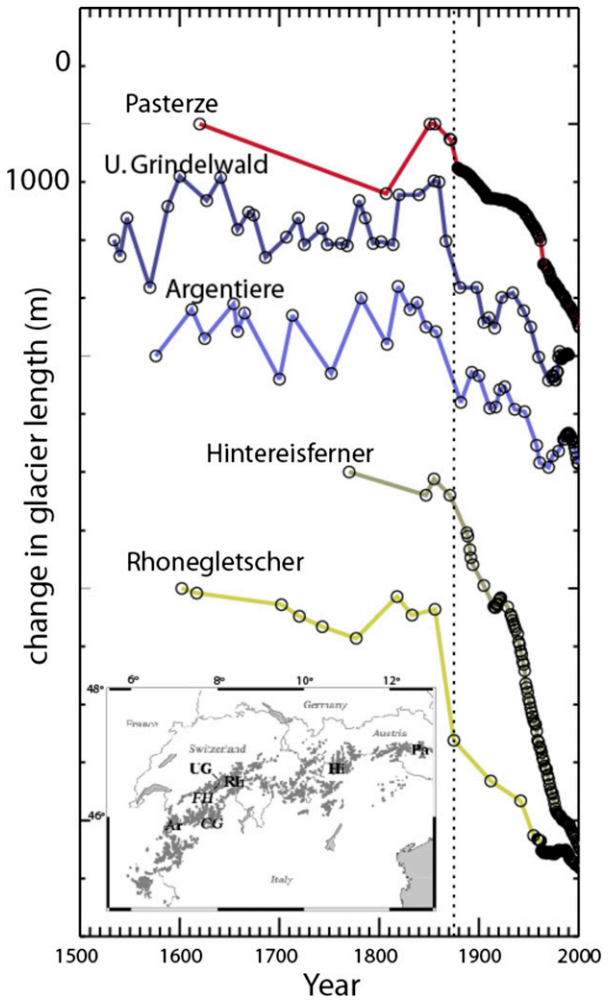

Fig. 1. Change in glacier length (m) relative to the first year of measurement for five Alpine glaciers (offset consecutively by 1,000 m for clarity). (*Inset*) The locations of Glacier d'Argentiere, Rhonegletscher, Unterer Grindelwaldgletscher, Pasterzegletscher and Hintereisferner, and Fiescherhorn and Colle Gnifetti ice cores. The underlying gray circles represent glacier locations in the Alps from the World Glacier Inventory (www.geo.unizh.ch/wgms).

the melt season will generally increase glacier melt and result in glacier retreat, reinforced by advected energy fluxes from recently exposed bare ground (14, 15). As indicated by Huybrechts et al. (10) and many others, our best understanding of changes in temperature and precipitation in the 19th century indicates that there was no regional climatic anomaly coincident with the coherent retreat of glaciers in the Alps near 1865. However, a known transition did occur across that half century and into the 20th century that may have held powerful potential consequences for absorption of solar radiation, earlier melt of snow cover and, in turn, the retreat of glaciers. That transition was the dramatic rise in a byproduct of industrialization: black carbon (BC).

Here we present the evidence and hypothesis that the rise in BC loading that began in the mid-19th century and its general increase to the mid-20th century increased the absorption of solar radiation by snow, caused earlier exposure of glacier ice and, in turn, increased mass losses and retreat of glaciers in the Alps.

Records of Black Carbon in Ice

BC and mineral dust can significantly reduce albedo of snow and ice through strong absorption of sunlight in the visible wavelengths (and at higher concentrations out into the near-infrared) (16) and, therefore, significantly affect glacier mass balance and regional to global climate (17–19). BC is now considered to be the second most potent climate warmer behind carbon dioxide (20, 21). In exposed settings, such as glaciers, net solar radiation accounts for the vast majority of the energy available for melt (19, 22). The increase in absorbed solar energy by BC in snow is usually greater than the reduction in absorbed solar energy by snow resulting from atmospheric BC+organic carbon (the component of carbonaceous aerosols that only weakly absorbs light) dimming (23), particularly

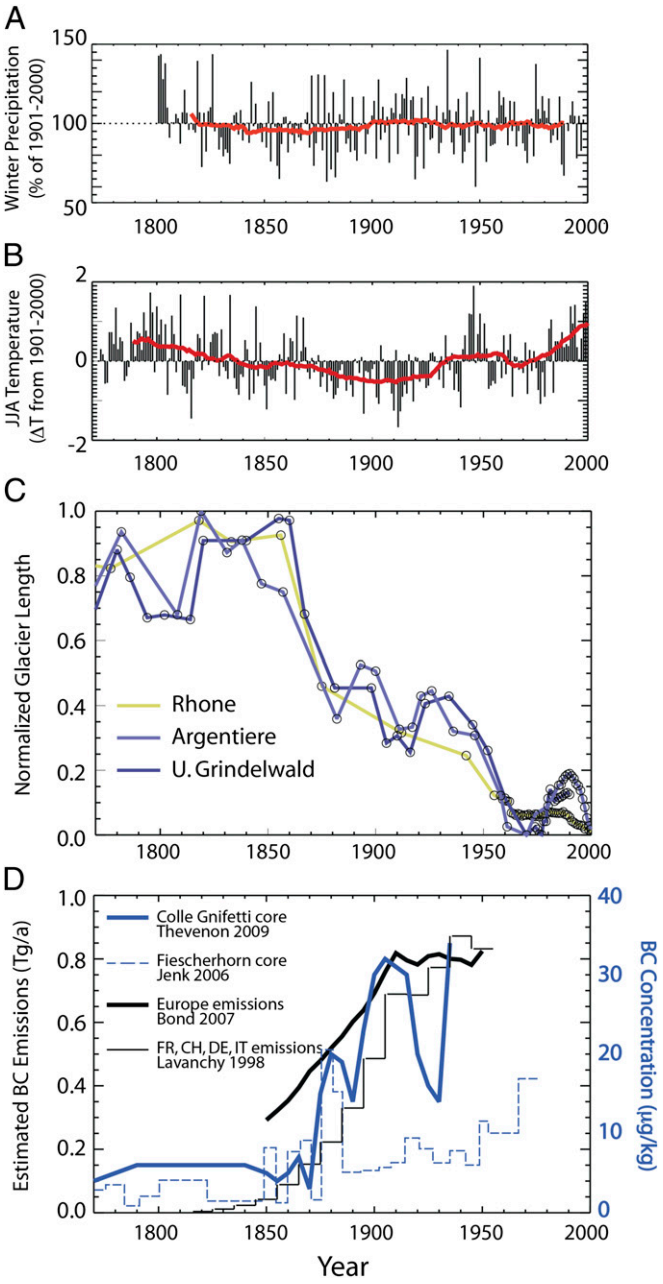

Fig. 2. (*A*) Precipitation percentage of the 1901–2000 mean from the Historical Instrumental Climatological Surface Time Series of the Greater Alpine Region (HISTALP) database (5) (with 30-y running mean). (*B*) Deviation of temperature from the 1901–2000 mean from the HISTALP database (with 30-y running mean). (*C*) Subset of glacier length variations normalized to the range of lengths across period 1800–2000. (*D*) BC concentrations in the Fiescherhorn ice core (26) and Colle Gnifetti ice core (27), and estimated BC emissions for Europe (24) and for France, Switzerland, Germany, and Italy (25).

in ablation zones where deposited particles can influence radiation for months beyond deposition. Moreover, although atmospheric BC can reduce at-surface irradiance, atmospheric heating by BC absorption ultimately warms the surface through sensible and latent heating exchanges (21).

The Industrial Revolution in Western Europe led to an increase in emissions of BC and other carbonaceous aerosols, starting in Great Britain in the mid-18th century, spreading to France in the early 19th century, and then to Germany and much of the rest of Western Europe by the mid-19th century (24). Estimates of historical emissions for Europe show that BC emissions increased dramatically after 1850 and did not decrease significantly until after 1970 (24) (Fig. 2). In particular, the Alps were surrounded by areas of intensive industrialization and BC emissions (24, 25). Ice cores extracted at high elevations in the European Alps (25–28) similarly reflect these increased emissions from Europe, with increased BC concentrations beginning between 1850 and 1870 and general increases thereafter until well into the 20th century (Fig. 2). It is these increases in BC concentrations and the associated radiative forcing in the snow and ice that may represent the additional energy required for the distinct retreat that began around 1865.

Summertime BC loading to the Colle Gnifetti glacier saddle (CG, elevation 4,455 m) on Monte Rosa in the Swiss–Italian Alps stepwise jumped from ~7 $\mu g \cdot kg^{-1}$ before 1850 to ~14 $\mu g \cdot kg^{-1}$ in the range 1850–1870, and maintained a general increase into the late 20th century (27), with a spike in the 1880s. Given that emissions were likely greater in winter/spring because of seasonal heating needs, the absolute magnitudes of BC deposition at the CG site should have been greater than the summertime values reported here.

Similarly, BC concentrations at the Fiescherhorn Glacier ice core site (FH, elevation 3,900 m), in the interior Swiss Alps, began to increase from a background of 3–4 $\mu g \cdot kg^{-1}$ around 1860–1870 and more than doubled to ~20 $\mu g \cdot kg^{-1}$ by 1880 (26). Concentrations roughly plateaued from then until the 1920s, when they dropped and then increased to ~30 $\mu g \cdot kg^{-1}$ by the 1940s (26).

Legrand et al. (28) suggest from analysis of the Col du Dome ice core (elevation 4,250 m on Mont Blanc, western end of the Alps) that BC did not increase until the 1930s (28). However, this core is markedly shorter than the CG or FH cores, reaching only back to ~1900 (28, 29). If one analyzed the CG and FH only from 1900 forward, those records would similarly suggest that an increase only began after World War II (25–27), yet the full temporal record shows a plateau across the first half of the 20th century that lies well above the pre-1860s concentrations. The temporally coincident concentrations at the Col du Dome are smaller than at the CG and FH. The relative remoteness of the western end of the Alps from industrial regions and techniques for retrieving BC may explain the differences (28). However, the Mer de Glace, in the valley immediately to the southwest from the Argentiere, experienced a similar abrupt retreat at 1860 (30).

Below, we estimate the radiative forcings by these changes in BC loading and whether they were of sufficient magnitude to produce the pronounced negative glacier mass balance that began in the mid-19th century.

Scaling High-Altitude BC Concentrations to Ablation Zones

Snowmelt in glacier ablation zones (elevations of 1,500–2,200 m before the glacier retreat began in earnest around 1860) (Fig. 1) completely removes each year's snow, eliminating the time series of deposition that is preserved in the high-elevation ice core sites. Consequently, we must infer aerosol loading in the ablation zones from higher-elevation ice core records and vertical scaling. Although we do not have ambient air-pollutant concentration data from the late 19th century, we argue by analogy to present day spatial distributions of anthropogenic pollution that the surface darkening and accelerated melting in the lower reaches of Alpine glaciers in the late 19th century would have been much greater than that indicated by the aerosol layers in the ice cores collected in the high-elevation sites.

Spatial patterns of combustion activity (and thus BC emissions) surrounding the Alps in the late 19th century were roughly parallel to those in the present period. This finding is confirmed at a continent-wide scale by the gridded historical emission patterns compiled by Bond et al. (24). Large population centers and major concentrations of industrial activities are confined to the valleys of the Po, Rhone, and Rhine rivers and their tributaries. Past and present communication lines follow those river systems, and links between them generally follow connecting mountain passes used since the late Roman Empire.

Beginning in the mid-19th century, rail systems in and around the Alps paralleled existing roads. Rail systems eventually became more extensive than the preexisting road network by the building of tunnels and, more importantly, the synergistic growth of rail transport and the tourism industry in the Alps. Together, these two factors greatly expanded the human footprint in the region (31–33), and consequently brought significant new emissions into close proximity with many of the regions' glaciers.

The most significant stationary pollution sources of the late 19th century were coal combustion for industry and coal and biomass fuels used for space heating (24). Transportation emissions in the late 19th century were dominated by coal-fired steam locomotives (24). Urban and industrial stationary combustion sources today are a mix of coal, petroleum, and natural gas with dramatically reduced emissions, with biomass heating restricted to smaller towns and rural areas. In transport, widespread electrification has nearly eliminated rail emissions, but a network of highways largely paralleling the rail corridors has replaced coal-transport emissions with motor vehicle exhaust. This similarity implies that modern air-quality patterns resemble past spatial distributions of air pollutants, and modern data can be used to infer past low- to midaltitude concentrations relative to the high-elevation ice core sites.

Meteorological analysis of the dispersion potential in these valleys shows persistent local temperature inversions with stable to highly stable air very common (34). Modeling studies indicate that upslope transport of pollutants is often blocked by downslope flow from above, especially if the upper slopes have a high albedo (as with snow or glacial ice), dispersing pollutants horizontally across the valley at that level. Pollutants generated outside the mountains may also be transported into the uplands and deposited there.

Spring and summer deposition to glacier ice is particularly important, as it occurs as the solar flux is peaking and as winter's protective cold (air temperature over the ice persistently below 0 °C) is waning. In spring to summer, solar heating drives turbulent afternoon mixing over the Alps (35), thus bathing the intermediate slopes (2- to 3-km elevation) of Alpine glaciers in local and regional aerosols at a time of year when deposited material will be exposed to sunlight on snow surfaces. With mixing to the highest altitudes limited by meteorological processes in winter, and only brief, intermittent exposure to the polluted boundary layer in summer, the highest terrain is effectively isolated from the magnitude of deposition that impacts glaciers at lower and middle altitudes.

Strong vertical gradients of pollution in alpine valleys are well documented (29, 34, 36–38). Metals associated with sources in the Chamonix and Maurienne valleys (Al, Fe, Ti) sampled in fresh snow show vertical gradients of a factor > 10 from valley floor to mountain crest (36). Observations using an instrumented aircraft show aerosol concentration gradients in excess of 30–1 between the valley floor and the surrounding peaks were observed in flight (37). Sulfate aerosols have vertical gradients in

the Alps of two orders-of-magnitude in winter and about one order-of-magnitude in summer (29).

At the snow surface, modern observations (1990s and 2000s) of BC concentrations in lower elevation snow (1,800–2,600 m) in the Alps confirm these gradients, with winter to spring means of ~120 $\mu g \cdot kg^{-1}$ to nearly 500 $\mu g \cdot kg^{-1}$ (17) compared with the ice core concentrations of 7 $\mu g \cdot kg^{-1}$ before 1850 and compared with the peaks of 20–35 $\mu g \cdot kg^{-1}$ in the ice core record. These more recent concentrations were observed when BC emissions are markedly lower than during the peak emissions of industrialization.

The bulk of evidence suggests that aerosol concentrations and deposition loading below 2,000 m is one-to-two orders-of-magnitude greater than above 4,000 m. Therefore, in the radiative-forcing calculations below, we bound the lower elevation radiative forcings with concentrations of 10- and 20-times the high-elevation concentrations. Ten-times provides a lower bound, below which is highly unlikely, and 20-times a conservative upper bound.

Radiative Forcing

Measurements of snow spectral albedo, snow and ice energy balance, and glacier mass balance were not made in the Alps or anywhere else for that matter until well into the 20th century, with some isolated stake measurements of accumulation and ablation starting in the late 19th century (39).

Therefore, we simulated radiative forcings from the increased late 19th century BC concentrations. We estimated snowmelt that would result from these radiative forcings and, by translating the BC radiative forcings into equivalent changes in atmospheric temperature, we can estimate anomalies in glacier mass balance with an established glacier model built on temperature and precipitation (16). The lack of detailed meteorological data, irradiance data, and deposition time series would render a more physically based modeling exercise largely useless because of uncertainties in dominant assumptions.

We estimated monthly and annual surface radiative forcings by BC in snow at the ice core sites and in the snow ablation zones from the CG and FH black carbon concentrations using the snow, ice, and aerosol radiative model (SNICAR) (17). The details of this modeling are provided in the *Supporting Information*. We bracket the radiative forcings and in turn estimate glacier mass balance with scenarios of scaling the ice core BC concentrations by 1-, 10-, and 20-times. We present the radiative-forcing differences from the respective mean background BC radiative forcings before 1850.

The increases in BC during the period 1850–1880 produced comparable magnitudes of radiative forcings between the two cores (Fig. 3), with the increase at the CG coming earlier than the FH by ~20 y (Fig. 2), a difference that lies just at the edge of the relative uncertainties in dating of the two cores (*Supporting Information*). The radiative forcings in the accumulation zones where the ice cores were extracted reached 3 $W \cdot m^{-2}$.

The mean annual radiative forcings at the FH in the ablation zone scenarios (10- to 20-times) reached 13 $W \cdot m^{-2}$ by 1880, and 22–23 $W \cdot m^{-2}$ in the period 1910–1940 (Fig. 3*A*). The CG mean annual radiative forcings in the ablation zone scenarios increased to 8–17 $W \cdot m^{-2}$ by 1880, and again to 9–18 $W \cdot m^{-2}$ by the 1970s (Fig. 3*B*). At the CG ablation zone, the snowmelt season (April/May/June, AMJ) radiative forcing peaked at 14–28 $W \cdot m^{-2}$ around 1880 and gradually increased from 3 to 8 $W \cdot m^{-2}$ in the early 1900s, until the marked rise in the 1970s to 14–33 $W \cdot m^{-2}$. At the FH ablation zone, AMJ radiative forcing rose steadily to a peak of 10–20 $W \cdot m^{-2}$ in the early 1900s and 19–38 $W \cdot m^{-2}$ at the end of the BC record in 1940. This magnitude of radiative forcing by dust in the Colorado River Basin has been shown to shorten snow cover duration by approximately 1 mo (40).

Further forcing would have come from earlier heating of surrounding talus/rock surfaces from earlier loss of snow cover (14, 15). These surfaces would heat rapidly because of their lower albedo and provide an additional long-wave emission to the snow surface and heating of the boundary layer, leading to increases in sensible heating of the snow and ice surfaces (14, 15).

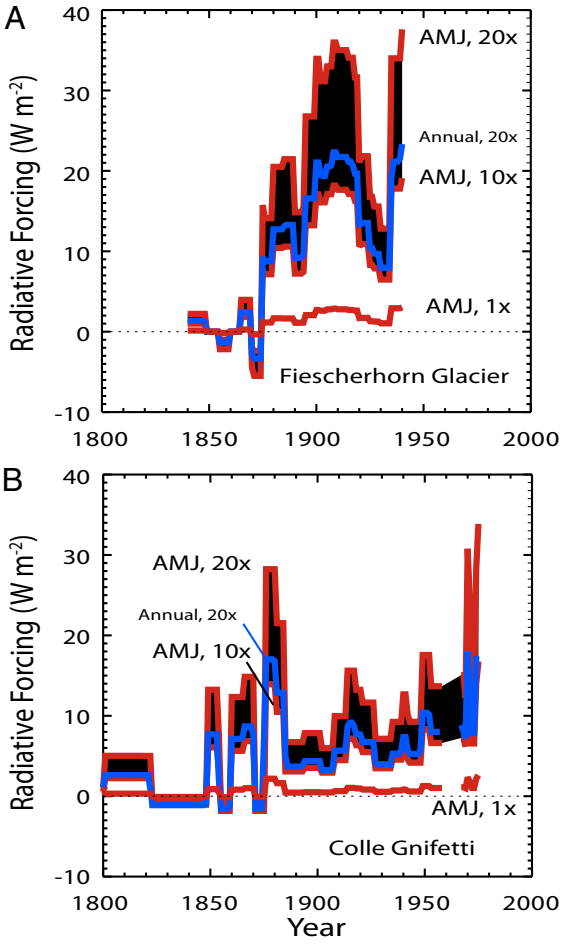

Fig. 3. Annual mean ablation zone (20-times), AMJ ablation zone (10- to 20-times, black shading), and AMJ accumulation zone radiative forcings. (*A*) Fiescherhorn; (*B*) Colle Gnifetti.

Influence on Simulated Glacier Mass Balance

We converted these forcings into mass of snow melted across the melt season AMJ. With the enthalpy of fusion of water at 0 °C of 0.334×10^6 $J \cdot kg^{-1}$, the 10–20 $W \cdot m^{-2}$ AMJ radiative forcing in 1880 at FH translates into 240–480 $kg \cdot m^{-2}$ of seasonal melt, or 0.6–1.2 m of a snow column of a typical melt season density 400 $kg \cdot m^{-3}$. By the early 20th century, AMJ radiative forcing of 19–38 $W \cdot m^{-2}$ increases melt by 450–890 $kg \cdot m^{-2}$ or 1.1–2.2 m of snow with density 400 $kg \cdot m^{-3}$ (0.4–0.9 m snow water equivalent). In the CG ablation scenario, the 1880 forcing of 14–28 $W \cdot m^{-2}$ melts 330–660 $kg \cdot m^{-2}$ of snow or 0.8–1.6 m of the snow column, whereas the 1900s forcings of 3–15 $W \cdot m^{-2}$ melts 70–350 $kg \cdot m^{-2}$ of snow or 0.2–0.9 m of the column, reaching 330–780 $kg \cdot m^{-2}$ and 0.8–1.9 m snow depth by the end of the record in the late 1970s (0.3–0.8 m snow water equivalent). Before the snowpack temperature was 0 °C, the radiative forcings would have accelerated snow warming and likewise increased sublimation losses of snow mass.

Surface mass balance anomalies are translated into glacier length as anomalies in the dynamic ice flow. To simulate these anomalies, detailed knowledge of the spatial distribution of the mass balance and its anomalies is necessary. Even in the

present, this is only possible to obtain by implementing an extensive measurement program to constrain the multitude of parameters necessary for modeling the spatial distribution of the surface energy fluxes. Although it is obvious that negative mass balance anomalies of the magnitude reconstructed here will eventually lead to negative glacier-length anomalies, a quantitative estimate of their timing and magnitude requires a large number of assumptions not inferable from existing environmental records, and so can only add qualitative uncertainty around the case for a strong influence of BC on glacier change.

Based on the work of Oerlemans (41) and Kuhn (42), we can translate changes in net shortwave radiation (radiative forcing by BC) into equivalent changes in free air temperature with respect to a common impact on glacier mass balance or move in equilibrium line altitude. These radiative-forcing equivalent changes in temperature are 10 and 18 $W{\cdot}m^{-2}\,°C^{-1}$, respectively (described in *Supporting Information*). We then use the monthly radiative-forcing equivalent change in temperatures (in the ablation zones, representing the glacier terminus) to perturb the glacier mass balance simulations of Marzeion et al. (13).

With glacier terminus temperature and precipitation under conditions of no BC forcing, this model simulates well the annual glacier mass balance in the latter half of the 20th century on the Hintereisferner (13), with an uncertainty estimate (root mean squared error) of ± 0.30 m water equivalent for years outside of the calibration period, based on a cross validation. On glaciers without mass balance measurements, uncertainties are estimated to be ± 0.67 m water equivalent (13). However, despite the accurate representation of glacier mass balance during the period of mass balance observations in the latter half of the 20th century, the climate-driven model does not exhibit the marked negative mass balance anomalies that would have been required to cause the range-wide decrease in glacier lengths that began around 1865 (Fig. 4). This inability to find the necessary negative mass balance anomalies is consistent with the other modeling studies described above that were driven by temperature and precipitation (8). As with those other studies, mass balance anomalies driven by temperature and precipitation alone in the period of 1850–1920 become increasingly positive (Fig. 4*A*).

However, when perturbed by the BC radiative-forcing equivalent changes in temperature derived from the BC content in the CG and FH ice cores, modeled mass balance anomalies become increasingly negative, consistent with the mid- to late-19th century glacier retreat and consistent with lack of direct temperature or precipitation forcing. The mean cumulative negative mass balances across all glaciers and the two scenarios of 10- and 20-times concentrations are about −15 m water equivalent by 1900 and −30 m water equivalent by 1930 (i.e., approximately −0.5 m water equivalent per y), with magnitudes and timing consistent with the observed retreat (Fig. 4*B*).

Different glacier geometries and ice dynamics cause a broad spectrum in length response to mass balance changes. However, volume-length scaling relationships (43) allow us to estimate the magnitude of a corresponding length change. For example, using these relationships, a thinning of 15–30 m of a glacier with an initial area of 10 km^2 translates to an eventual retreat of 1.6–3.0 km. Such a retreat would not occur instantaneously, and would be dampened by reduced mass loss once the lowest-lying ice is lost (44, 45). Based on a linear model and accounting for the stabilizing effect of glacier retreat to higher altitudes, Roe (46) estimates the equilibrium length response of an idealized glacier similar (but smaller) in size to the glaciers investigated here to be −2.5 km for a mass balance anomaly of −2 m water equivalent per y^{-1}.

Based on our model result of a BC forced mass balance anomaly of approximately −0.5 m water equivalent per y^{-1}, this would eventually translate to about 600-m length retreat and presumably more, given the sustained elevated magnitude of BC forcing above preindustrialization and the size difference between the idealized

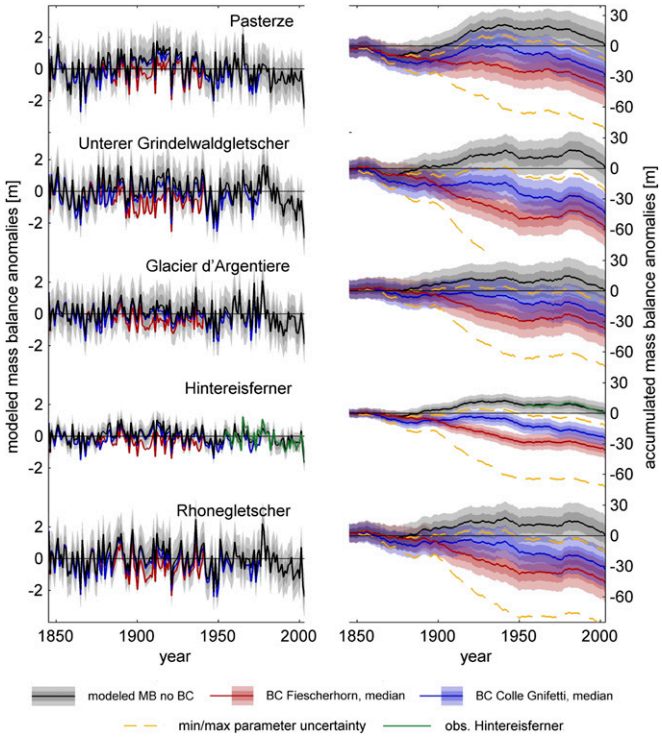

Fig. 4. (*Left*) Black: modeled mass balance anomalies without BC forcing, dark shading indicates one/light shading indicates two SEs; red: BC atmospheric temperature equivalent forcing from Fiescherhorn reconstruction; blue: BC atmospheric temperature equivalent forcing from Colle Gnifetti reconstruction. (*Right*) Black: accumulated mass balance (MB) anomalies without BC forcing; red: accumulated mass balance anomalies simulated with BC temperature equivalent from Fiescherhorn reconstruction; blue: accumulated mass balance anomalies simulated with BC atmospheric temperature equivalent from Colle Gnifetti reconstruction; dark shading indicates one/light shading indicates two accumulated SEs of the accumulated mass balance anomalies. Mass balance anomalies shown are the median values obtained from an ensemble of simulations performed for each glacier, covering the BC forcing parameter uncertainty range (see *Supporting Information* for details). Orange: maximum and minimum of the accumulated mass balance anomalies of the entire ensemble (FH and CG combined). Green: observed mass balance anomalies of Hintereisferner.

glaciers and the glaciers considered here. The observed retreats from ∼1860 to ∼1930 for the five glaciers shown in Fig. 1 were 670 m (Argentiere), 450 m (Unterer Grindelwald), 1,030 m (Hintereis), 670 m (Pasterze), and 1,590 m (Rhone). Even the minimum BC impact on glacier mass balance is outside of two SEs of the mass balance model most of the time on most glaciers. Therefore, BC very likely played a significant role in the glacier retreat.

Discussion

The magnitudes and timing of radiative forcing by BC in snow are consistent with the "additional features affecting the glacier's mass balance that are not captured well in the ambient climatic records," suggested by Huybrechts et al. (10). Even the conservatively low forcing scenario described above indicates negative mass balance occurring with realistic timing. Radiative forcing by increasing deposition of BC is unique in explaining the Alps glacier retreat from the LIA in the mid-19th century while maintaining consistency with the temperature and precipitation reconstructions. The BC hypothesis is not refuted by any available records, or by the calculations presented here. This impact of BC on glacier mass balance in the Alps pushes our understanding of the onset of anthropogenic influence back further than CO_2 forcing alone would indicate.

The greatest focus of the end of the LIA is often afforded to the European Alps because of the quality, density, and duration of measurements of climate variables and the relative quality of measurements of glacier lengths back 400+ y. Our hypothesis of BC radiative forcing here is specific to the end of the LIA in the Alps. Across the globe however, despite the common mistaken impression that all glaciers began to retreat in 1850, the end of the glacial LIA was asynchronous, as was regional climate. For example, glaciers in Southern Norway had high stands that ranged from 1750 to the early 1900s (47), whereas the best available records for southern South America suggest that the bulk of retreat in Argentina did not occur until the early 1900s (48). In the Bolivian Andes, moderate glacier retreat began after 1740 (49). Himalayan glaciers have been in a general state of retreat since the mid 1800s (50). The potential implication of BC deposition in the end of the glacial LIA in the European Alps and the growing understanding of the magnitude of radiative forcing by dust and BC suggests that studies of past, present, and future changes in glacier mass balance should consider these albedo-driven changes to ensure physical consistency.

ACKNOWLEDGMENTS. We thank Johannes Oerlemans and Florian Thevenon for access to data. Part of this work was performed at the Jet Propulsion Laboratory, California Institute of Technology under a contract with the National Aeronautics and Space Administration. This research was funded by National Science Foundation Grant ATM-0432327 (to T.H.P.); National Aeronautics and Space Administration Project NNX10AO97G (to T.H.P.); National Science Foundation Grant ATM-0852775 (to M.G.F.); and Austrian Science Fund (FWF): P22443-N21 (to B.M.).

1. Grove JM (2004) *Little Ice Ages: Ancient and Modern* (Routledge, London), p 718.
2. Vincent C, Meur EL, Six D (2005) Solving the paradox of the end of the Little Ice Age in the Alps. *Geophys Res Lett* 32(9):L09706.
3. Zemp M, Haeberli W, Hoelzle M, Paul F (2006) Alpine glaciers to disappear within decades? *Geophys Res Lett* 33(13):L13504.
4. Zumbühl HJ, Steiner D, Nussbaumer SU (2008) 19th century glacier representations and fluctuations in the central and western European Alps: An interdisciplinary approach. *Global Planet Change* 60(1–2):42–57.
5. Auer I, et al. (2007) HISTALP—Historical instrumental climatological surface time series of the Greater Alpine Region. *Int J Climatol* 27(1):17–46.
6. Casty C, Wanner H, Luterbacher J, Esper J, Böhm R (2005) Temperature and precipitation variability in the European Alps since 1500. *Int J Climatol* 25(14):1855–1880.
7. Oerlemans J (2005) Extracting a climate signal from 169 glacier records. *Science* 308(5722):675–677.
8. Kerschner H (1997) Statistical modelling of equilibrium-line altitudes of Hintereisferner, central Alps, Austria, 1859-present. *Ann Glaciol* 24:111–115.
9. Greuell W (1992) Hintereisfirner, Austria: Mass-balance reconstruction and numerical modelling of the historical length variations. *J Glaciol* 38(129):233–244.
10. Huybrechts P, de Nooze P, Decleir H (1989) Numerical modeling of Glacier d'Argentiere and its historical front variations. *Glacier Fluctuations and Climatic Change*, ed Oerlemans J (Kluwer Academic, The Netherlands), pp 373–389.
11. Schmeits MJ, Oerlemans J (1997) Simulation of the historical variations in length of Unterer Grindelwaldgletscher, Switzerland. *J Glaciol* 43(143):152–164.
12. Stroeven A, van de Wal R, Oerlemans J (1989) Historic front variations of the Rhone Glacier: Simulation with an ice flow model. *Glacier Fluctuations and Climatic Change*, ed Oerlemans J (Kluwer Academic, The Netherlands), pp 391–405.
13. Marzeion B, Hofer M, Jarosch AH, Kaser G, Mölg T (2012) A minimal model for reconstructing interannual mass balance variability of glaciers in the European Alps. *The Cryosphere* 6:71–84.
14. Oerlemans J (1986) Glaciers as indicators of a carbon dioxide warming. *Nature* 320: 607–609.
15. Olyphant G, Isard SA (1988) The role of advection in the energy balance of late-lying snowfields: Niwot Ridge, Front Range, Colorado. *Water Resour Res* 24(11):1962–1968.
16. Hadley OL, Kirchstetter TW (2012) Black-carbon reduction of snow albedo. *Nature Climate Change* 2:437–440.
17. Flanner MG, Zender CS, Randerson JT, Rasch PJ (2007) Present-day climate forcing and response from black carbon in snow. *J Geophys Res* 112(D11):2481–2497.
18. Hansen J, Nazarenko L (2004) Soot climate forcing via snow and ice albedos. *Proc Natl Acad Sci USA* 101(2):423–428.
19. Painter TH, et al. (2007) Impact of disturbed desert soils on duration of mountain snow cover. *Geophys Res Lett* 34(12):L12502.
20. Bond TC, et al. (2013) Bounding the role of black carbon in the climate system: A scientific assessment. *J Geophys Res* 118(11):5380–5552.
21. Ramanathan V, Carmichael G (2008) Global and regional climate changes due to black carbon. *Nat Geosci* 1:221–227.
22. Oerlemans J (2000) Analysis of a 3 year meteorological record from the ablation zone of Morteratschgletscher, Switzerland: Energy and mass balance. *J Glaciol* 46(155): 571–579.
23. Flanner MG, et al. (2009) Springtime warming and reduced snow cover from carbonaceous particles. *Atmos Chem Phys* 9:2481–2497.
24. Bond TC, et al. (2007) Historical emissions of black and organic carbon aerosols from energy-related combustion, 1850–2000. *Global Biogeochem Cycles* 21(2):GB2018.
25. Lavanchy VMH, Gaggeler HW, Schotterer U, Schwikowski M, Baltensperger U (1999) Historical record of carbonaceous particle concentrations from a European high-alpine glacier (Colle Gnifetti, Switzerland). *J Geophys Res* 104(D17):21227–21236.
26. Jenk TM, et al. (2006) Radiocarbon analysis in an Alpine ice core: Record of anthropogenic and biogenic contributions to carbonaceous aerosols in the past. *Atmos Chem Phys* 6:5381–5390.
27. Thevenon F, Anselmetti FS, Bernasconi SM, Schwikowski M (2009) Mineral dust and elemental black carbon records from an Alpine ice core (Colle Gnifetti glacier) over the last millennium. *J Geophys Res* 114(D17):1–11.
28. Legrand M, et al. (2007) Major 20th century changes of carbonaceous aerosol components (EC, WinOC, DOC, HULIS, carboxylic acids, and cellulose) derived from Alpine ice cores. *J Geophys Res* 112(D23):1–12.
29. Schwikowski M (2004) Reconstruction of European air pollution from alpine ice cores. *Earth Paleoenvironments: Records Preserved in Mid- and Low-Latitude Glaciers*, ed Cecil LD (Kluwer Academic, The Netherlands), pp 95–119.
30. Nussbaumer SU, Zumbühl HJ, Steiner D (2007) Fluctuations of the Mer de Glace (Mont Blanc area, France) AD 1500–2050: An interdisciplinary approach using new historical data and neural network simulations, Vol 40, pp 1–183.
31. Barker ML (1982) Traditional landscape and mass tourism in the Alps. *Geogr Rev* 72(4): 395–415.
32. Pawson E, Egli H-R (2001) History and (re)discovery of the European and New Zealand Alps until 1900. *Mt Res Dev* 21(4):350–358.
33. Piskunov VN (2009) Parameterization of aerosol dry deposition velocities onto smooth and rough surfaces. *Aerosol Science* 40(8):664–679.
34. Brulfert G, et al. (2006) Assessment of 2010 air quality in two Alpine valleys from modelling: Weather type and emission scenarios. *Atmos Environ* 40(40):7893–7907.
35. Nyeki S, et al. (2000) Convective boundary layer evolution to 4 km asl over high-Alpine terrain: Airborne lidar observations in the Alps. *Geophys Res Lett* 27(5):689–692.
36. Dumolard P (2009) Road transport and atmospheric pollution—Northern French Alps case. *Present Enviroment and Sustainable Development* 3:5–20.
37. Chazette P, et al. (2005) Three-dimensional survey of pollution during winter in French Alps valleys. *Atmos Environ* 39(6):1035–1047.
38. Cui J, et al. (2011) Free tropospheric ozone changes over Europe as observed at Jungfraujoch (1990–2008): An analysis based on backward trajectories. *J Geophys Res* 116(D10):D10304.
39. Zemp M, Hoelzle M, Haeberli W (2009) Six decades of glacier mass-balance observations: A review of the worldwide monitoring network. *Ann Glaciol* 50(50): 101–111.
40. Painter TH, Skiles SM, Deems JS, Bryant AC, Landry CC (2012) Dust radiative forcing in snow of the Upper Colorado River Basin: Part I. A 6 year record of energy balance, radiation, and dust concentrations. *Water Resour Res* 48(7):1–14.
41. Oerlemans J (2001) *Glaciers and Climate Change* (Swets and Zeitlinger, Lisse), p 148.
42. Kuhn M (1981) Climate and glaciers. *Sea Level, Ice and Climatic Change*, ed Allison I (IAHS, Wallingford), Vol 131, pp 3–20.
43. Bahr DB, Meier M, Peckham S (1997) The physical basis of glacier volume-area scaling. *J Geophys Res* 102(B9):355–362.
44. Marzeion B, Jarosch AH, Gregory JM (2013) Feedbacks and mechanisms affecting the global sensitivity of glaciers to climate change. *The Cryosphere* Discussions 7:2761–2800.
45. Paul F (2010) The influence of changes in glacier extent and surface elevation on modeled mass balance. *The Cryosphere* 4:569–581.
46. Roe G (2011) What do glaciers tell us about climate variability and climate change? *J Glaciol* 57(203):567–578.
47. Nussbaumer SU, Nesje A, Zumbuhl H (2011) Historical glacier fluctuations of Jostedalsbreen and Folgefonna (southern Norway) reassessed by new pictorial and written evidence. *Holocene* 21(3):455–471.
48. Masiokas MH, et al. (2009) Glacier fluctuations in extratropical South America during the past 1000 years. *Palaeogeogr Palaeoclimatol Palaeoecol* 281(3–4):242–268.
49. Rabatel A, Francou B, Jomelli V, Naveau P, Grancher D (2008) A chronology of the Little Ice Age in the tropical Andes of Bolivia (16 °S) and its implications for climate reconstruction. *Quat Res* 70(2):198–212.
50. Mayewski PA, Jascheke PA (1979) Himalaya and trans Himalaya glacier fluctuations since AD 1812. *Arct Alp Res* 11(3):267–287.